Full-dimensional multi configuration time dependent Hartree calculations of the ground and vibrationally excited states of He2,3Br2 clusters

Álvaro Valdés, Rita Prosmiti, Pablo Villarreal, and Gerardo Delgado-Barrio

Citation: J. Chem. Phys. **135**, 054303 (2011); doi: 10.1063/1.3618727
View online: http://dx.doi.org/10.1063/1.3618727
View Table of Contents: http://jcp.aip.org/resource/1/JCPSA6/v135/i5
Published by the American Institute of Physics.

Full-dimensional multi configuration time dependent Hartree calculations of the ground and vibrationally excited states of $He_{2,3}Br_2$ clusters

Álvaro Valdés,[a] Rita Prosmiti, Pablo Villarreal, and Gerardo Delgado-Barrio
Instituto de Física Fundamental (IFF-CSIC), CSIC, Serrano 123, 28006 Madrid, Spain

(Received 3 June 2011; accepted 5 July 2011; published online 1 August 2011)

Quantum dynamics calculations are reported for the tetra-, and penta-atomic van der Waals He_NBr_2 complexes using the multiconfiguration time-dependent Hartree (MCTDH) method. The computations are carried out in satellite coordinates, and the kinetic energy operator in this set of coordinates is given. A scheme for the representation of the potential energy surface based on the sum of the three-body $HeBr_2$ interactions at CSSD(T) level plus the He-He interaction is employed. The potential surfaces show multiple close lying minima, and a quantum description of such highly floppy multiminima systems is presented. Benchmark, full-dimensional converged results on ground vibrational/zero-point energies are reported and compared with recent experimental data available for all these complexes, as well as with previous variational quantum calculations for the smaller $HeBr_2$ and He_2Br_2 complexes on the same surface. Some low-lying vibrationally excited eigenstates are also computed by block improved relaxation calculations. The binding energies and the corresponding vibrationally averaged structures are determined for different conformers of these complexes. Their relative stability is discussed, and contributes to evaluate the importance of the multiple-minima topology of the underlying potential surface. © *2011 American Institute of Physics*. [doi:10.1063/1.3618727]

I. INTRODUCTION

The first experiments on van der Waals (vdW) clusters consisting of a dihalogen molecule and rare-gas atoms have been performed by Levy *et al.*,[1,2] followed by a large number of studies on systems such as He_nI_2 (n=1–3),[3,4] Ne_nI_2 (n=1–6),[2,5,6] Ne_nBr_2,[7] $Rg_{1,2}X_2$ (Rg=He, Ne, Ar and X=Cl, Br),[8–11] Ne_nICl (n=1–5),[12,13] He_nICl ((n=1–3).[14,15] More recently the interest in studying such species has been intensified due to additional experiments, rotational, and infrared spectroscopy on doped helium nanodroplets,[16–18] and on small/intermediate-sized doped helium clusters.[19]

Despite the fact that experimental data are available over the last 30 years, the theoretical treatment of such systems is still a significant challenge. For the triatomic complexes exact full-dimensional quantum calculations of the dynamics are feasible,[20–23] with limitations imposed by the accuracy of the assumed potential surface. Recently high quality *ab initio* potential energy surfaces (PESs) have been calculated for such triatomic species,[20,24–30] and attempts have also been made using pairwise three-body interaction potentials to represent the PESs of larger complexes.[31–35] Thus the first issue in this context, from the theoretical side, is how to properly describe the multidimensional potential energy surface or, in other words, at what extent the usual assumption of additive forces holds. Reported *ab initio* results have been shown that for He_2Br_2 system, the pairwise atom-atom interactions are not able to describe the PES of the complex, while a sum of three-body $HeBr_2$ terms,[29] plus the He–He interaction, can accurately represent the interaction energies for this cluster.[34] This latter has been also supported by recent experimental data on $He_{2,3}Br_2$, $He_{2,3}ICl$, and Ne_2Br_2 complexes.[14,36] In particular, laser-induced fluorescence and two-laser action spectra have been recorded, and different isomers for these vdW clusters have been stabilized and identified.[14] The assignment of the spectroscopic features to multiple conformers associates them to configurations of the system with the He atoms localized to linear and/or T-shape wells of the corresponding PES. These findings have been found to be in accord with predictions made by previous theoretical investigations for the tetra-atomic clusters.[31,34]

The work presented here expands our previous efforts to evaluate the multidimensional surfaces of such vdW complexes obtained from first principles *ab initio* computations, by direct comparison with the experiment. In this way we can study the role of uncertainties in the PES on the spectroscopic and dynamic properties of these systems. This involves full-dimensional exact quantum dynamics simulations, which as the number of intermolecular degrees of freedom increases are getting computationally difficult, or impossible for the larger complexes. Thus, such calculations for small clusters (two or three He atoms), where experimental data are available, can serve as benchmark for approximate treatments[37,38] in order to deal with larger species, and provide with required information, such as input data, for such approaches.[39]

Up to date reduced five dimensional (5D) variational calculations have been carried for the He_2Br_2 on the PES of Ref. 34, which includes three-body terms. Also by using a semiempirical pairwise HeBr potential surface quantum-chemistry-like treatments analogous to Hartree,[37,38] configuration-interaction,[40] and full-configuration-interaction[41] calculations, in electronic structure methodology have been also reported for larger systems up to $N = 60$, $N = 5$, and $N = 4$, respectively. In spite of the theoretical

[a]Electronic mail: alvaro.v@iff.csic.es.

efforts to develop new methods for handling such systems, in applications for He_NBr_2 only simple pairwise PESs have been employed. Although, as it has been shown[9,14,29,34] multibody potential terms are very important for an accurate representation of the PESs of the triatomic and tetra-atomic clusters of this series. Therefore, in order to achieve a satisfactory understanding of the spectroscopy and dynamics of these systems accurate quantum-dynamics simulations are needed employing reasonable accurate potential surfaces.

In this work we take advantage of the reliable representation of the He_NBr_2 potential, and the availability of performing a full-dimensional (6D and 9D) quantum treatment within the multiconfiguration time dependent Hartree (MCTDH) framework.[42–44] This method expands the wave function in a basis of time-dependent wave functions (single-particle functions (SPFs)), which in principle allows the treatment of more degrees of freedom than many other quantum dynamics methods, while maintaining correlation between motion in the different degrees of freedom, and has been applied to study dynamics of multidimensional systems.[45,46] From the MCTDH calculations the zero-point energies, some low-lying vibrational states, and the properties of the ground state conformer, as well as the ones of different isomers of the He_NBr_2 complexes, with N=1,2,3, are reported and discussed.

The structure of the article is as follows: in Sec. II we describe the representation of the potential energy surface, kinetic energy operator, and the computational details of the MCTDH calculations. In Sec. III we present the results of these calculations for the ground and low-lying vibrational states of the He_NBr_2 complexes, with N=1, 2, 3, together with their comparison with experimental data and previous theoretical estimates. Finally, the conclusions are presented in Sec. IV.

II. METHODOLOGY AND COMPUTATIONAL DETAILS: BOUND STATE CALCULATIONS

The molecular Hamiltonian of the He_N–Br_2 systems in the BF satellite coordinates ($\mathbf{r}$,$\mathbf{R_k}$), where $\mathbf{r}$ is the vector joining the two Br atoms and $\mathbf{R_k}$ are the vectors from the center of mass of the Br_2 molecule to the $k = 1, \ldots, N$ He atoms, can be written as

$$\hat{H} = -\frac{\hbar^2}{2m}\frac{\partial^2}{\partial r^2} + \frac{\mathbf{j}^2}{2mr^2} + \sum_{k=1}^{N}\left(-\frac{\hbar^2}{2\mu}\frac{\partial^2}{\partial R_k^2} + \frac{\mathbf{l_k^2}}{2\mu R_k^2}\right) - \frac{\hbar^2}{m_{Br_2}}\sum_{k<l}\nabla_k\cdot\nabla_l + V(\mathbf{r}, \mathbf{R_1}, \ldots, \mathbf{R_N}), \quad (1)$$

where $\mathbf{j}$ and $\mathbf{l_k}$ are the angular momenta associated to the vectors $\mathbf{r}$ and $\mathbf{R_k}$, respectively, m is the reduced mass of the diatomic Br_2 molecule, μ is the reduced mass of the He-Br_2 system, and m_{Br_2} is two times the mass of one Br atom. By performing 5D variational calculations for He_2–Br_2, the effect of the kinetic energy coupling terms ($-\hbar^2/m_{Br_2}\sum_{k<l}\nabla_k\cdot\nabla_l$) was found to be of less than 0.02 cm^{-1} in the energy for the five lowest bound states. Thus, for the low-lying states for which we are interested in these terms can be neglected.[47–49]

A. Potential form

It has been shown that, for the He_2Br_2 tetra-atomic molecule a potential form consisting in the sum of the three-body $HeBr_2$ interactions plus the He–He interaction is able to describe very accurately the 5D tetra-atomic *ab initio* CCSD(T) potential.[34] In this work we extend that potential form to penta-atomic He_3–Br_2 molecules, and include the dependence in the bondlength distance of the Br_2 molecule,

$$V(\mathbf{r}, \mathbf{R_1}, \ldots, \mathbf{R_N}) = \sum_k V_{HeBr_2}(\mathbf{r}, \mathbf{R_k}) + \sum_{k<l} V_{He-He}(\mathbf{R_k}, \mathbf{R_l}) + U_{Br_2}(\mathbf{r}), \quad (2)$$

where the corresponding $V_{HeBr_2}(\mathbf{r}, \mathbf{R_k})$ terms are the CCSD(T) parametrized potential of the $HeBr_2$ complex,[29] the $V_{He-He}(\mathbf{R_k}, \mathbf{R_l})$ terms are the potential function for He_2 given in Ref. 50, and $U_{Br_2}(\mathbf{r})$ is the diatomic interaction Br-Br potential.[51]

It has been established, from both experiment and theory, that the PESs of rare gas-dihalogen complexes support a double-minima topology, corresponding to linear and T-shaped configurations for their electronic ground states. We used the sets of coordinates (r, R_3, θ_3), (r, R_1, R_3, θ_1, θ_3, φ_1), and (r, R_1, R_2, R_3, θ_1, θ_2, θ_3, φ_1, φ_2) shown in Fig. 1 to describe the $HeBr_2$, He_2Br_2, and He_3Br_2 systems, respectively. We label the different equilibrium geometries as (#T, #L) following the notation of Boucher and co-workers,[14] where #T and #L are the number of He atoms in the T-shape and linear geometries, respectively. Using the potential form of Eq. (2) we have calculated the optimal geometries for the He_NBr_2 complexes with N=1, 2, and 3 and in Table I- we present the geometry and energy of the optimal structures found for these complexes. For the triatomic case the minimum of the potential corresponds to a linear (0,1) structure with energy of −48.70 cm^{-1} followed by a T-shape configuration at −40.19 cm^{-1}. The three most stable minima for the tetra-atomic He_2Br_2 molecule correspond to linear (0,2), police-nightstick (1,1), and tetrahedral (2,0) structures with well-depths of −97.41, −89.11, and −88.07 cm^{-1}, respectively. For the He_3Br_2 the first three minima of the potential, corresponding to the (1,2), (2,1), and (3,0) conformers,

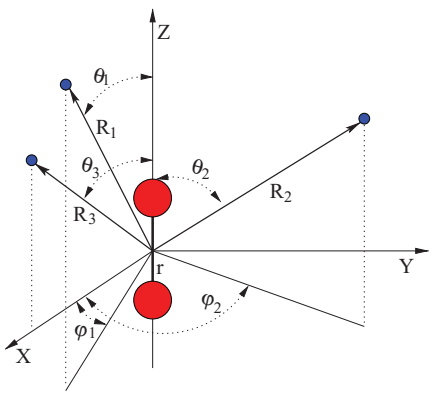

FIG. 1. Schematic representation of coordinate system for He_3Br_2 complex.

TABLE I. Potential well-depths (D_e in cm^{-1}) and equilibrium distances (R_e in angstroms and φ_i^e in degrees) for the different (#T,#L) minima of the He_NBr_2 systems, with N=1,2,3 and r_e= 2.281 Å.

(#T,#L)	D_e	R_i^e	φ_i^e
(0,1)	48.70	4.41	–
(1,0)	40.19	3.58	–
(0,2)	97.41	4.41 / 4.41	–
(1,1)	89.11	3.58 / 4.41	–
(2,0)	88.07	3.58 / 3.58	48.6
(1,2)	138.05	3.58 / 4.41 / 4.41	– / –
(2,1)	137.22	3.58 / 3.58 / 4.41	48.6 / –
(3,0)	136.28	3.58 / 3.58 / 3.58	48.6 / 97.1

are very close in energy, within less than 2 cm^{-1}, at energies of −138, 05, −137.22, and −136.28 cm^{-1}, respectively. In Fig. 2 various contour plot cuts for the He_3Br_2 system are presented. In Fig. 2(a) two of the He atoms and the two Br atoms are frozen in the tetra-atomic linear (0,2) equilibrium configuration while the remaining He atom is allowed to move; in Figs. 2(b) and 2(c) the frozen atoms are in the tetra-atomic police-nightstick (1,1) equilibrium positions, and in Fig. 2(d) they are fixed in the tetra-atomic (2,0) configuration with the He atoms in the equilibrium positions of Table I and the Br_2 bondlength fixed at r_e =2.281 Å. Besides the three minima mentioned above, these plots reveal some other possible equilibrium structures that, being higher in energy, are not detailed further here. In Table II we show a comparison of the CCSD(T) interaction energies[52] using effective core potentials (ECP) with different basis sets for Br and He atoms, with the potential values obtained from the analytical form (see Eq. (2)) for the above mentioned configurations. For the small-core ECPs a series of correlation consistent basis sets are available, and this allows to extrapolate the energies to the (approximate) complete basis set (CBS) limit. We have performed an extrapolation of the correlation energies using the mixed Gaussian/exponential three-point form proposed by Peterson *et al.*,[53] $E_X = E_{\rm CBS} + Ae^{-(X-1)} + Be^{-(X-1)^2}$, where X is the cardinal number, and the series of aug-cc-pVTZ, aug-cc-pVQZ, and aug-cc-pV5Z basis sets was employed. As it can be seen in Table II the extrapolated interaction energies of the extrapolation scheme of the small-core calculations are lower than the ones from the analytical form, and show small differences between the different (#T, #L) structures, especially for the He_3Br_2 complex.

In order to make the MCTDH method efficient, the potential energy operator must be written as a sum of products of single-particle operators. There exists an efficient approach within the MCTDH package, called POTFIT, to obtain the desired product representation by expanding the PES in natural potentials.[54,55] In Table III we present the parameters used for the POTFIT calculations. We include the type of primitive basis functions where *sin* stands for the sine *discrete variable representation* (DVR) basis, *HO* stands for the harmonic oscillator DVR basis, and *Leg* and *Pleg* stands for the one and two dimensional Legendre DVR basis, respectively.[42] The number of primitive basis functions and the number of natural potentials included in the POTFIT calculations performed for the V_{HeBr_2} and V_{He-He} potential energy surfaces are also included. As φ_3 is set to 0 (see Fig. 1), we had to perform different fittings of the V_{He-He} potential in the penta-atomic case to consider all the He-He interactions. The introduction of weights can increase the accuracy of the potential fit for the relevant regions, where the weight is 1 while for the other points the weight value of 0 is given. In Table III we list the relevant regions of the potential considered in the

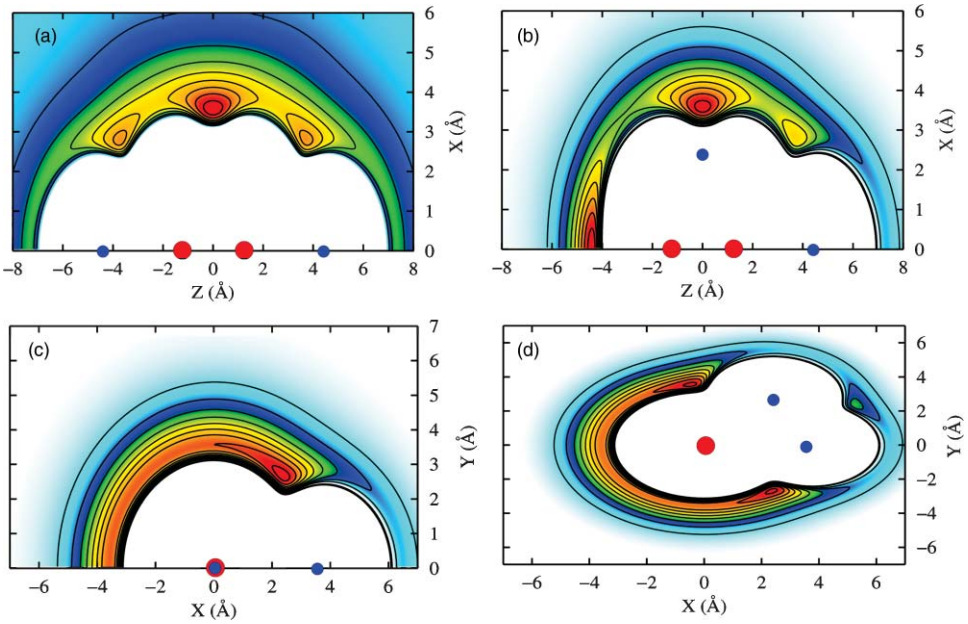

FIG. 2. Contour plots of the He_3Br_2 potential energy surface, $V(r, R_1, R_2, R_3, \theta_1, \theta_2, \theta_3, \varphi_1, \varphi_2)$ in the ZX (a and b) and XY (c and d) Cartesian planes. The Br_2 distance is fixed at 2.281 Å along the Z-axis, while the geometry of the tetra-atomic molecule is fixed to a linear (0,2) configuration (a), police-nightstick (1,1) configuration (b and c), and tetrahedral (2,0) configuration (d) with the He atoms in the equilibrium positions of Table I. Contour intervals are of 5 cm^{-1} for energies from 135 to 80 cm^{-1}.

TABLE II. CCSD(T) interaction energies and their complete basis set limit values using small-core ECP10MDF pseudopotentials in conjunction with the indicated AVXZ-PP and AVXZ (with X=T, Q, and 5) basis sets for Br atoms and He atoms, respectively. B stands for a bending configuration of one of the He-atoms (see Fig. 2(a)).

	CCSD(T)/ECP10MDF				
(#T,#L)	AVTZ-PP/AVTZ	AVQZ-PP/AVQZ	AV5Z-PP/AV5Z	CBS[TQ5]	PES Eq. (2)
(0,1)	−38.98	−45.21	−47.83	−49.36	−48.70
(1,0)	−32.29	−37.92	−40.39	−41.83	−40.19
(0,2)	−78.06	−90.41	−95.63	−98.68	−97.41
(1,1)	−71.54	−83.39	−88.44	−91.39	−89.11
(2,0)	−71.21	−82.99	−88.22	−91.27	−88.07
(1,2)	−110.89	−128.84	−136.46	−140.91	−138.05
(2,1)	−110.73	−128.72	−136.49	−141.02	−137.22
(3,0)	−110.58	−128.41	−136.34	−140.97	−136.28
(B,2)	−101.29	−116.89	−123.59	−127.50	−126.80

different calculations mentioned above, and we also include the root mean square (rms) error for the fits we obtained.

B. MCTDH: improved relaxation calculations

To perform the calculation of the rovibrational levels we use the *improved relaxation* and *block improved relaxation* methods implemented in the Heidelberg MCTDH code.[42–44] We first obtain a good starting vector for each isomer using the *block improved relaxation* method to compute the ground and first excited states of a multidimensional system. In these calculations we do not consider the parity under $\mathbf{R_i} \leftrightarrow \mathbf{R_j}$ inversion so for tetra-atomic and penta-atomic cases we obtain a bunch of degenerated states. Besides, some vibrational excited states corresponding to He–He stretching modes in the T-shaped well arrangements configurations are calculated. Some of lowest lying states of each configuration are chosen as starting vectors for the *improved relaxation* calculations to achieve a better convergence of the results.

The Hamiltonian for zero total angular momentum ($J = 0$) in the coordinates described above for N=1 and 2 is presented in Refs. 20, 46, respectively. For the N=3, the Hamiltonian without the cross terms takes the form,[56–58]

$$\begin{aligned}\hat{H}_{He_3-Br_2} = &-\frac{1}{2m}\frac{\partial^2}{\partial r^2} + \sum_{k=1}^{3}\left(-\frac{1}{2\mu}\frac{\partial^2}{\partial R_k^2}\right)\\ &-\sum_{k=1}^{3}\left(\frac{1}{2\mu R_k^2}+\frac{1}{2mr^2}\right)\left(\frac{\hbar^2}{\sin^2\theta_k}\frac{\partial}{\partial\theta_k}\sin\theta_k\frac{\partial}{\partial\theta_k}\right)\\ &-\sum_{l=1}^{2}\left(\frac{1}{2\mu R_l^2}+\frac{1}{2mr^2}\right)\frac{\hbar^2}{\sin^2\theta_l}\frac{\partial^2}{\partial^2\varphi_l}\\ &-\left(\frac{1}{2\mu R_3^2}+\frac{1}{2mr^2}\right)\frac{\hbar^2}{\sin^2\theta_3}\end{aligned}$$

TABLE III. Parameters used in the POTFIT program. We include for each coordinate its range, the number of the primitive basis sets and the type of them. The number of natural potentials (see text) the relevant regions of the potential considered and the rms error for the fits are also listed. Contr indicates the mode over which a contraction is performed.

	$HeBr_2(r,R_3,\theta_3)$	He-He(R_1,R_3,θ_1,θ_3,φ_1)	He-He(R_1,R_2,θ_1,θ_2,φ_1,φ_2)
	Primitive basis		
N_r (sin)	35	–	–
r-range (Å)	[2.1, 2.46]	–	–
N_R (HO)	41	41	41
R-range (Å)	[2.80, 7.41]	[2.80, 7.41]	[2.80, 7.41]
N_θ (Leg)/N_θ (Pleg)	21 / 0	21 / 21	0 / 21
θ-range (radian)	$[0, \pi]$	$[0, \pi]$	$[0, \pi]$
N_ϕ	–	15	15
ϕ-range (radian)	$[0, 2\pi]$	$[0, 2\pi]$	$[0, 2\pi]$
	Natural potentials		
N_r	20	–	–
N_R	20	12	16
N_θ	Contr	12	–
$N_{\theta,\phi}$	–	Contr	Contr/100
Relevant regions	V < 20 cm^{-1}	V < 16 cm^{-1}	V < 6 cm^{-1}
rms error on relevant Grid points (cm^{-1})	$< 10^{-3}$	0.4	0.4

TABLE IV. Number of SPF and least populated orbital population of the MCTDH *improved relaxation* calculations.

	$HeBr_2$	He_2Br_2	He_3Br_2
SPF			
N_r	1	1	1
N_{R_3}	10	–	–
N_{R_1,R_3}	–	18	–
N_{R_1,R_2,R_3}	–	–	12
N_θ	10	16	6
$N_{\theta,\phi}$	–	34	28
Least populated orbital population	1×10^{-12}	1×10^{-6}	0.5×10^{-5}

$$
\begin{aligned}
&\times \left(\frac{\partial^2}{\partial^2 \varphi_1} + 2\frac{\partial^2}{\partial \varphi_1 \partial \varphi_2} + \frac{\partial^2}{\partial^2 \varphi_2} \right) \\
&+ \frac{\hbar^2}{mr^2} \left(\frac{\partial^2}{\partial^2 \varphi_1} + \frac{\partial^2}{\partial \varphi_1 \partial \varphi_2} + \frac{\partial^2}{\partial^2 \varphi_2} \right) \\
&+ \frac{\hbar^2}{mr^2} \left\{ -\cos(\varphi_1 - \varphi_2) \frac{\partial^2}{\partial \theta_1 \partial \theta_2} \right. \\
&- \cos\varphi_1 \frac{\partial^2}{\partial \theta_1 \partial \theta_3} - \cos\varphi_2 \frac{\partial^2}{\partial \theta_2 \partial \theta_3} \\
&+ \cot\theta_3 \sin\varphi_1 \frac{\partial^2}{\partial \theta_1 \partial \varphi_1} + \cot\theta_3 \sin\varphi_2 \frac{\partial^2}{\partial \theta_2 \partial \varphi_2} \\
&+ [\cot\theta_2 \sin(\varphi_2 - \varphi_1) + \cot\theta_3 \sin\varphi_1] \frac{\partial^2}{\partial \theta_1 \partial \varphi_2} \\
&+ [\cot\theta_1 \sin(\varphi_1 - \varphi_2) + \cot\theta_3 \sin\varphi_2] \frac{\partial^2}{\partial \theta_2 \partial \varphi_1} \\
&+ \cot\theta_1 \sin\varphi_1 \frac{\partial^2}{\partial \theta_3 \partial \varphi_1} + \cot\theta_2 \sin\varphi_2 \frac{\partial^2}{\partial \theta_3 \partial \varphi_2} \\
&+ \cot\theta_1 \cot\theta_3 \cos\varphi_1 \frac{\partial^2}{\partial \varphi_1^2} \\
&+ \cot\theta_2 \cot\theta_3 \cos\varphi_2 \frac{\partial^2}{\partial \varphi_2^2} \\
&+ \left[\cot\theta_1 \cot\theta_3 \cos\varphi_1 + \cot\theta_2 \cot\theta_3 \cos\varphi_2 \right. \\
&\left. \left. - \cot\theta_1 \cot\theta_2 \cos(\varphi_2 - \varphi_1) \right] \frac{\partial^2}{\partial \varphi_1 \varphi_2} \right\} \\
&+ V(r, R_1, R_2, R_3, \theta_1, \theta_2, \theta_3, \varphi_1, \varphi_2). \qquad (3)
\end{aligned}
$$

The primitive basis used in the MCTDH calculations is the same as for the POTFIT calculations (see Table III). In Table IV we resume the number of SPFs included in the *improved relaxation* calculations for He_NBr_2 with $N = 1,2,3$. In order to speed up the calculations we performed convergence tests on the number of SPFs. For the degree of freedom corresponding to the Br-Br distance one SPF function is enough to described the lowest vdW states. The population of a second SPF on this degree of freedom was found to be of less than 10^{-5} for *improved relaxation* calculations of the ground van der Waals states of the He_2Br_2 and He_3Br_2 complexes. The populations of the highest (least populated) natural orbital of the other modes is included for the three cases in Table IV. The improved relaxation runs are converged to within 10^{-3} cm^{-1}.

III. RESULTS AND DISCUSSION

In Table V we present the energy and average structure values for the lowest bound states of the complexes He_NBr_2 with $N = 1,2,3$, together with the calculated zero-point energies for each system. One can see that these complexes are highly anharmonic with the zero point energies (ZPE) to count for more than 65% of the corresponding potential well-depth energy (see Table I). The results for the triatomic complex are given as a check. The lowest $HeBr_2$ vdW state corresponds to a linear (0,1) isomer with energy of -16.04 cm^{-1}, very close in energy to the T-shape (1,0) isomer (-14.92 cm^{-1}). These results are consistent with the experimental values of the binding energy of 17.0(8) and 16.6(8) cm^{-1} for the (0,1) and (1,0) isomers, respectively.[9] Also, they are in good agreement with previous 3D variational calculations[29] included in Table V.

For the tetra-atomic case, exact 5D variational calculations with the Br-Br distance frozen in its equilibrium value ($r_e = 2.28$ Å) predicted the existence of three stable conformers very close in energy corresponding to the (0,2), (1,1), and (2,0) configurations.[34] In this work, we extend this study by

TABLE V. Vibrationally averaged structures (R_1^0, R_2^0, R_3^0), ZPE, and binding energies (D_0) for the different He_NBr_2 isomers, with N=1,2,3. The comparison with experimental observations (Ref. 9) and previous theoretical results (Refs. 29, 34) is also included. Distances are in angstroms and energies are in cm^{-1}.

	$R_1^0/R_2^0/R_3^0$	ZPE(%)	D_0		
(#T,#L)		This work		Theor.	Expt.
(0,1)	4.87	32.66(67.06%)	16.035	16.02[a] (Ref. 29)	17.0(8)
(1,0)	4.13	–	14.920	14.90[a] (Ref. 29)	16.6(8)
(0,2) (5D/6D)	4.87 / 4.87	65.20(66.94%)	32.237 / 32.207	32.240[b] (Ref. 34)/ –	–
(1,1) (5D/6D)	4.77 / 4.23	–	31.483 / 31.216	31.437[b] (Ref. 34)/ –	33.6(1.1)
(2,0) (5D/6D)	4.11 / 4.11	–	30.859 / 30.286	30.930[b] (Ref. 34)/ –	33.2(1.1)
(1,2)	4.15 / 4.87 / 4.88	90.70(65.70%)	47.350	–	–
(2,1)	4.11 / 4.87 / 4.12	–	46.778	–	–
(3,0)	4.11 / 4.11 / 4.11	–	45.785	–	–

including the dependence in r (see Fig. 1). In Table V we report the energy and average structure values of the three isomers calculated with the MCTDH method using 5D and 6D calculations. We can see that the agreement between the 5D variational and MCTDH calculations is very good with a largest deviation of 0.07 cm^{-1} for the (2,0) isomer. Concerning the 6D calculations we can see that, although the r-dependence does not change the relative stability between the different isomers, it reduces the binding energy. The effect is larger for the tetrahedral (2,0) structure (0.57 cm^{-1}) than for the police-nightstick (1,1) isomer (0.27 cm^{-1}), being the smallest effect for the tetrahedral (2,0) structure with only 0.03 cm^{-1}. The larger influence of the r-dependence in the T-shape over the linear structures has been previously reported for $HeBr_2$ and HeI_2.[20,29,30]

Experimental data obtained from the two-laser action spectra measurements by Boucher *et al*. have identified two isomers for the He_2Br_2, the (1,1) and the (2,0) ones, while they did not observe any spectroscopic feature associated to the (0,2) conformer. This is most likely due to the spectral congestion when exciting the linear conformer to the highly delocalized intermolecular vibrational levels in the excited state, as they are very close in energy.[9] Further, in these studies, the analysis of the pressure and temperature dependence indicates the higher stability of the (1,1) isomer with respect to the (2,0), as predicted by the 5D variational calculations[29] and confirmed in this work by the 6D MCTDH results (see Table V). The binding energy of the different isomers is 32.21, 31.22, and 30.29 cm^{-1}, for the (0,2), (1,1), and (2,0) isomers, respectively. In Fig. 3 we plot the angular and radial distribution probabilities in $\theta_{1,3}$, φ_1, and $R_{1,3}$ of the (0,2), (1,1), and (2,0) states. We add a subindex to the legends indicating which of the He atoms we are considering.

We should note that there is no direct measurement of the binding energies of the tetra-atomic complex. However, based on a sum of the experimental values of the binding energy of the linear (0,1) and T-shape (1,0) triatomic conformers, Boucher *et al*. proposed binding energies of 33.6(1.1) and 33.2(1.1) cm^{-1} for the (1,1) and (2,0) He_2Br_2 complexes, respectively.[9] According to our calculations, the assumption of neglecting the He-He interaction does not affect the relative stability of the different conformers, with differences between the 6D result and the sum of the theoretical triatomic binding energies (see Table V) of 0.14, 0.26, and 0.45 cm^{-1} for the (0,2), (1,1), and (2,0) isomers, respectively. However, it has been shown that this assumption fails for systems such as He_2I_2, where the competition of the smaller differences between the linear and T-shape triatomic binding energies and the rotational effects results in a change of the relative stability of the isomers.[35]

Concerning the penta-atomic He_3Br_2 complex, our 9D calculations (see Fig. 1) support the experimental observation of three different conformers with (1,2), (2,1), and (3,0) geometries.[9] The one dimensional distributions in $\theta_{1,2,3}$ and in $R_{1,2,3}$, and the two dimensional distributions in φ_1 and φ_2, presented in Figs. 4–6 allow the assignment of the calculated bound states with binding energies of 47.35, 46.78, and 45.76 cm^{-1} to the (1,2), (2,1), and (3,0) isomers, respectively (see Table V). In Fig. 4 we plot the angular density distributions in θ_1, θ_2, and θ_3 of the He_3Br_2 (1,2), (2,1), and (3,0) states in the top, central, and bottom panels, respectively. Looking at the figure, the assignment of the states to the different conformers is straightforward. In the top panel the distribution of one He atom is centered at 90° while the other ones are located in the linear region; in the middle panel only one He atom is in the linear region while in the bottom panel the three atoms are centered in the T-shape well. Also, in Fig. 5, we display the radial density probabilities. The ones in the top panel correspond to one He atom in the

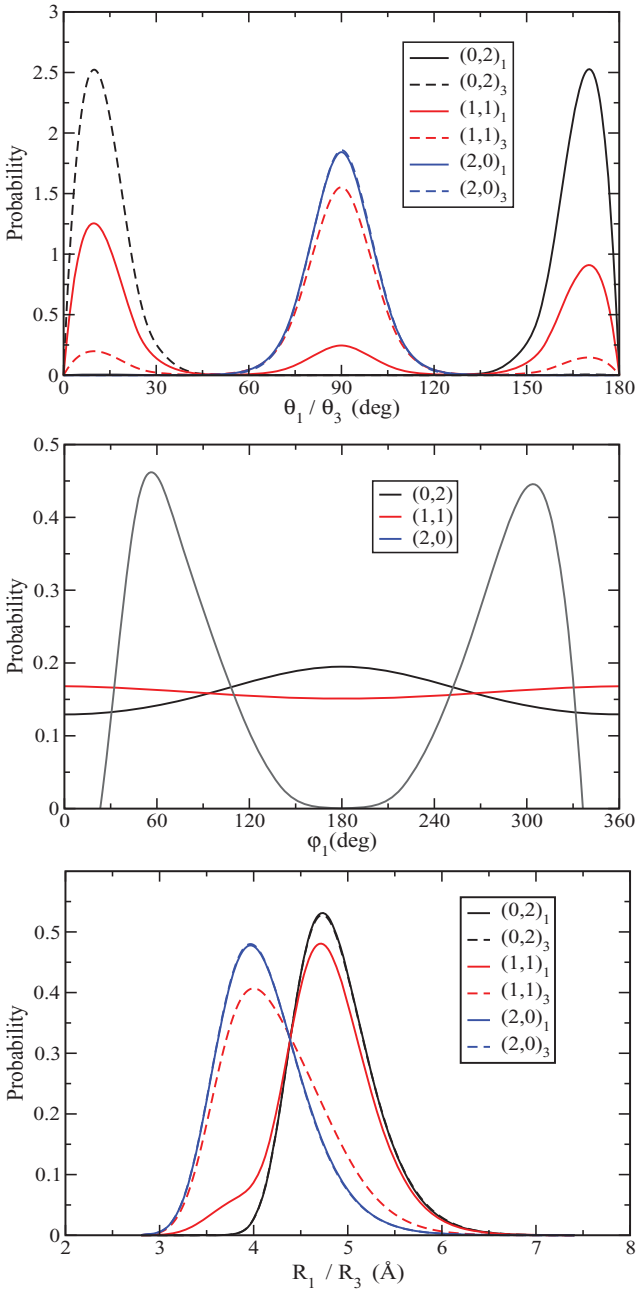

FIG. 3. Angular and radial probability density distributions of the indicated He_2Br_2 (0,2), (1,1), and (2,0) conformers, respectively. The set of coordinates used to describe the He_2Br_2 complex is (r, R_1, R_3, θ_1, θ_3, φ_1) (see Fig. 1). In the top and bottom panels we add a subindex to the legends indicating if we are considering the He_1 (solid lines) or the He_3 (dashed lines). In the top panel, we plot the distributions in $\theta_{1,3}$, in the central panel in φ_1, and in the bottom panel in $R_{1,3}$.

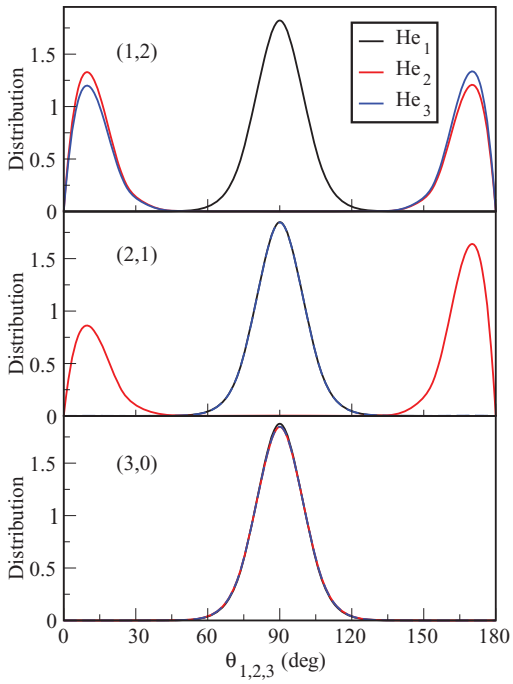

FIG. 4. Probability density distributions in θ_1 (black/solid), θ_2 (red/gray), and θ_3 (blue/dashed) in degrees of the He_3Br_2 (1,2), (2,1), and (3,0) conformers in the top, central, and bottom panels, respectively.

T-shape region (R_0=4.1 Å, see Table V) and two He atoms in the linear regions (R_0=4.9 Å). The central panel distributions correspond to two tetrahedral He atoms and one He atom in the linear configuration and the bottom panel shows all three He atoms in the T-shape well. Finally, in Fig. 5 one can see a planar distribution in φ_1 and φ_2 in the top panel, where the He

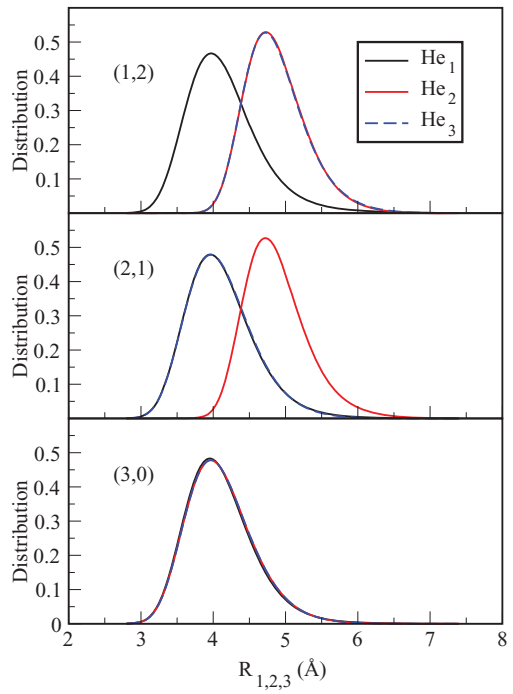

FIG. 5. Probability density distributions in R_1 (black/solid), R_2 (red/gray), and R_3 (blue/dashed) in angstroms of the He_3Br_2 (1,2), (2,1), and (3,0) conformers in the top, central, and bottom panels, respectively.

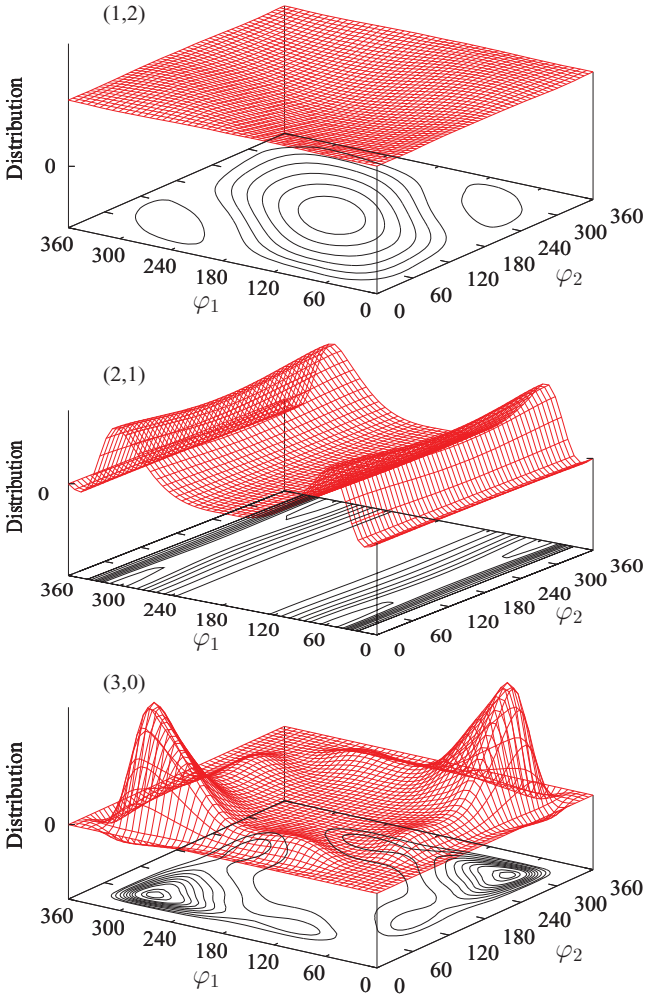

FIG. 6. Two dimensional angular density distributions in φ_1 and φ_2 in degrees of the He_3Br_2 (1,2), (2,1), and (3,0) conformers in the top, central, and bottom panels, respectively.

atoms defining these angles are in the linear positions while the remainder He atom is in the T-shape region, (see Fig. 1). In the other two panels, two (central panel) or three (bottom panel) He atoms are interacting in the T-shape region, where the probability densities present a much more structured distribution.

Unfortunately, there is no experimental information about the energetic ordering of the conformers or estimations of their binding energies. Moreover, according to our results, the difference between the sum of the triatomic $HeBr_2$ binding energies and the calculated penta-atomic binding energies increases to 0.36, 0.90, and 1.03 cm^{-1}, for the (1,2), (2,1), and (3,0) conformers, respectively. Using a sum of two-body terms semiempirical PES and a configuration-interaction approach to the variational calculations Felker obtained several bound states of the He_NBr_2 systems, with $N = 1$–5.[40] However, the three-body interactions are essential to correctly describe the high anisotropy of the PES of systems composed of rare gas atoms and dihalogen molecules[20,29,30] and a pairwise additive potential fails to describe the linear structures. For He_2Br_2 and He_3Br_2, the ground states obtained by Felker[40] correspond to tetrahedral (2,0) and (3,0) structures with

energies about 8 cm^{-1} below the conformers involving He atoms in the linear well, in contradiction with the experimental observation of the coexistence of different conformers very close in energy, so no further comparison with their results is included here.

IV. CONCLUSIONS

The vdW $He_{2,3}Br_2$ clusters are studied by quantum dynamics full dimensional method, using the MCTDH approach. The PESs employed in the calculations are based on the sum of 3-body $HeBr_2$ terms plus the He–He ones. Such multibody interactions are necessary to model accurately the potential surface of these highly fluxional nature systems. The PES for each cluster is represented in a computationally adequate way for the quantum dynamical MCTDH calculations, by incorporating natural potential fits. Several low vibrational states of the tetra- and penta-atomic clusters are obtained using the improved relaxation and block improved relaxation techniques, available in the MCTDH package. By analyzing the vibrationally averaged structures of these states we could characterize multiple isomers for $He_{2,3}Br_2$ complexes, associated with (#T,#L) configurations, that have the He atoms localized in the T-shaped and linear potential wells.

The ZPE of these systems and the binding energies of the different conformers are calculated. The present results are compared with previous variational calculations for the tetra-atomic complex on the same PES, as well as with recent experimental data available for both 4- and 5-atomic clusters. In particular,

1. The MCTDH results show excellent agreement with previous 5D variational quantum calculations for the He_2Br_2. The reported values with MCTDH lie within 0.07 cm^{-1} from the reported variational data. The linear (0,2) isomer is found to be the most stable isomer, with the (1,1) and (2,0) ones to be 0.99 and 1.92 cm^{-1}, respectively, higher in energy.
2. The effect of the r dependence on the low-vibrational states is found to be very small, between 0.03 to 0.57 cm^{-1}, on the energies values without any influence on their relative order. As in the triatomic complexes the energy of the T-shaped conformers are more affected.
3. For the He_3Br_2 the fully converged 9D MCTDH calculations show that the vibrational ground state corresponds to a (1,2) conformer, while the next two states are related to the (2,1) and (3,0) isomers.
4. By comparing with the experimental data available on the binding energies and ordering of the different isomers a very good accord is found. Specifically, for the tetra-atomic He_2Br_2 system a quantitative agreement within 1.5 cm^{-1} is obtained, while for the penta-atomic He_3Br_2 we have a qualitative agreement since the three isomers, namely (1,2), (2,1), and (3,0), have been experimentally identified, although their binding energies and stability are not reported. We should also mention that the deviations with respect to the experimental estimates is to be partially attributed to the modified version of the band-shift rule that has been adopted by the experiment to support these assignments. On the other hand, we should point out that the predicted binding energies calculated here are for zero temperature of the system, while temperatures of 0.4–1.25 K have been reported for the experimental measurements, thus another, probably more important, source for the disagreement with the experimental energies could be the rotational excitation of the complex. Regarding now to the absence of any spectroscopic feature associated to the linear (0,2) He_2Br_2 isomer, we should mention that by taking into account the Franck-Condon factors, together with the topology of the X, and B excited states of such complexes, then the transitions between vdW levels with T-shaped character are strongly favored, while the ones involving linear states are less intense and blue-shifted. Depending now from the temperature, rotational excitation is also present in the experimental data, and thus the analysis and assignment is getting more difficult, especially for the linear ones.

The accuracy of the present full-dimensional quantum calculations is also limited by the uncertainties in the potential energy surfaces. The results obtained here are the most detailed description of the lower vibrational states of the $He_{2,3}Br_2$ vdW clusters. The validity of the potential energy form is established by comparison with the experimental data, that demonstrates the quality of the PESs and the importance of the three-body interactions for these systems. However, further experimental and theoretical efforts focusing on the spectroscopy and dynamics of such weakly bound complexes are necessary in order to complement the characterization and evaluation of the multidimensional PESs.

ACKNOWLEDGMENTS

The authors thank to Centro de Calculo (IFF), CTI (CSIC), and CESGA for allocation of computer time. This work has been supported by DGICYT, Spain, Grant No. FIS2010-18132. We also would like to thank O. Roncero for helpful discussions.

[1] R. E. Smalley, L. Wharton, and D. H. Levy, J. Chem. Phys. **68**, 671 (1978).
[2] J. A. Blazy, B. M. DeKoven, T. D. Russell, and D. H. Levy, J. Chem. Phys. **72**, 2439 (1980).
[3] W. Sharfin, K. E. Johnson, L. Wharton, and D. H. Levy, J. Chem. Phys. **71**, 1292 (1979).
[4] S. E. Ray, A. B. McCoy, J. J. Glennon, J. P. Darr, E. J. Fesser, J. R. Lancaster, and R. A. Loomis, J. Chem. Phys. **125**, 164314 (2006).
[5] M. Gutmann, D. M. Willberg, and A. H. Zewail, J. Chem. Phys. **97**, 8048 (1992).
[6] A. Burroughs, G. Kerenskaya, and M. C. Heaven, J. Chem. Phys. **115**, 784 (2001).
[7] B. A. Swartz, D. E. Brinza, C. M. Western, and K. C. Janda, J. Phys. Chem. **88**, 6272 (1984).
[8] S. R. Hair, J. I. Cline, C. R. Bieler, and K. C. Janda, J. Chem. Phys. **90**, 2935 (1989).
[9] D. S. Boucher, D. B. Strasfeld, R. A. Loomis, J. M. Herbert, S. E. Ray, and A. B. McCoy, J. Chem. Phys. **123**, 104312 (2005).
[10] A. Rohrbacher, N. Halberstadt, and K. Janda, Annu. Rev. Phys. Chem. **51** (2000).
[11] J. M. Pio, W. E. van der Veer, C. R. Bieler, and K. C. Janda, J. Chem. Phys. **128**, 134311 (2008).
[12] J. C. Drobits and M. I. Lester, J. Chem. Phys. **86**, 1662 (1987).

[13]D. B. Strasfeld, J. P. Darr, and R. A. Loomis, Chem. Phys. Lett. **397**, 116 (2004).
[14]D. S. Boucher, J. P. Darr, D. B. Strasfeld, and R. A. Loomis, J. Phys. Chem. A **112**, 13393 (2008).
[15]D. S. Boucher, M. D. Bradke, J. P. Darr, and R. A. Loomis, J. Phys. Chem. A **107**, 6901 (2003).
[16]S. Grebenev, J. P. Toennies, and A. F. Vilesov, Science **279**, 2083 (1998).
[17]K. Nauta and R. E. Miller, Science **287**, 293 (2000).
[18]J. P. Toennies and A. F. Vilesov, Angew. Chem., Int. Ed. **43**, 2622 (2004).
[19]J. Tang and A. R. W. McKellar, J. Chem. Phys. **119**, 5467 (2003).
[20]L. Garcia-Gutierrez, L. Delgado-Tellez, A. Valdés, R. Prosmiti, P. Villarreal, and G. Delgado-Barrio, J. Phys. Chem. A **113**, 5754 (2009).
[21]A. A. Buchachenko, R. Prosmiti, C. Cunha, G. Delgado-Barrio, and P. Villarreal, J. Chem. Phys. **117**, 6117 (2002).
[22]R. Prosmiti, C. Cunha, A. A. Buchachenko, G. Delgado-Barrio, and P. Villarreal, J. Chem. Phys. **117**, 10019 (2002).
[23]Á. Valdés, R. Prosmiti, P. Villarreal, G. Delgado-Barrio, D. Lemoine, and B. Lepetit, J. Chem. Phys. **126**, 244314 (2007).
[24]R. Prosmiti, C. Cunha, P. Villarreal, and G. Delgado-Barrio, J. Chem. Phys. **116**, 9249 (2002).
[25]R. Prosmiti, P. Villarreal, and G. Delgado-Barrio, Chem. Phys. Lett. **359**, 473 (2002).
[26]Á. Valdés, R. Prosmiti, P. Villarreal, and G. Delgado-Barrio, Chem. Phys. Lett. **375**, 328 (2003).
[27]R. Prosmiti, Á. Valdés, P. Villarreal, and G. Delgado-Barrio, J. Phys. Chem. A **108**, 6065 (2004).
[28]Á. Valdés, R. Prosmiti, P. Villarreal, G. Delgado-Barrio, and H.-J. Werner, J. Chem. Phys. **126**, 204301 (2007).
[29]Á. Valdés, R. Prosmiti, P. Villareal, and G. Delgado-Barrio, Mol. Phys. **102**, 2277 (2004).
[30]L. Delgado-Tellez, A. Valdés, R. Prosmiti, P. Villarreal, and G. Delgado-Barrio, J. Chem. Phys. **134**, 214304 (2011).
[31]Á. Valdés, R. Prosmiti, P. Villarreal, and G. Delgado-Barrio, J. Chem. Phys. **125**, 014313 (2006).
[32]M. P. de Lara-Castells, R. Prosmiti, G. Delgado-Barrio, D. López-Durán, P. Villarreal, F. A. Gianturco, and J. Jellinek, Phys. Rev. A **74**, 053201 (2006).
[33]C. Diez-Pardos, Á. Valdés, R. Prosmiti, P. Villarreal, and G. Delgado-Barrio, Theor. Chem. Acc. **118**, 511 (2007).
[34]Á. Valdés, R. Prosmiti, P. Villarreal, and G. Delgado-Barrio, J. Chem. Phys. **122**, 044305 (2005).
[35]A. Valdés, P. Barragán, R. P. de Tudela, J. S. Medina, L. Delgado-Tellez, and R. Prosmiti, "A theoretical characterization of multiple isomers of the He_2I_2 complex," Chem. Phys. (in press).
[36]J. M. Pio, M. A. Taylor, W. E. van der Veer, C. R. Bieler, J. A. Cabrera, and K. C. Janda, J. Chem. Phys. **133**, 014305 (2010).
[37]M. P. de Lara-Castells, D. López-Durán, G. Delgado-Barrio, P. Villarreal, C. Di Paola, F. A. Gianturco, and J. Jellinek, Phys. Rev. A **71**, 033203 (2005).
[38]D. López-Durán, M. P. de Lara-Castells, G. Delgado-Barrio, P. Villarreal, C. D. Paola, F. A. Gianturco, and J. Jellinek, Phys. Rev. Lett. **93**, 053401 (2004).
[39]C. Di Paola, F. A. Gianturco, D. López-Durán, M. P. de Lara-Castells, G. Delgado-Barrio, P. Villarreal, and J. Jellinek, ChemPhysChem **6**, 1348 (2005).
[40]P. M. Felker, J. Chem. Phys. **125**, 184313 (2006).
[41]M. de Lara-Castells, P. Villarreal, G. Delgado-Barrio, and A. Mitrushchenko, Int. J. Quantum Chem. **111**, 406 (2011).
[42]G. A. Worth, M. H. Beck, A. Jäckle, and H.-D. Meyer, the MCTDH package, version 8.2, 2000; H.-D. Meyer, version 8.3, 2002; version 8.4, 2007, see http://mctdh.uni-hd.de.
[43]H.-D. Meyer, U. Manthe, and L. S. Cederbaum, Chem. Phys. Lett. **165**, 73 (1990).
[44]M. H. Beck, A. Jäckle, G. A. Worth, and H.-D. Meyer, Phys. Rep. **324**, 1 (2000).
[45]O. Vendrell, M. Brill, F. Gatti, D. Lauvergnat, and H.-D. Meyer, J. Chem. Phys. **130**, 234305 (2009).
[46]C. Meier and U. Manthe, J. Chem. Phys. **115**, 5477 (2001).
[47]P. Villarreal, O. Roncero, and G. Delgado-Barrio, J. Chem. Phys. **101**, 2217 (1994).
[48]M. Hernández, A. Garcia-Vela, J. Campos-MartÃ-nez, O. Roncero, P. Villarreal, and G. Delgado-Barrio, Comput. Phys. Commun. **145**, 97 (2002).
[49]A. García-Vela, J. Rubayo-Soneira, G. Delgado-Barrio, and P. Villarreal, J. Chem. Phys. **104**, 8405 (1996).
[50]R. A. Aziz and M. J. Slaman, J. Chem. Phys. **94**, 8047 (1991).
[51]C. Cunha, R. Prosmiti, P. Villarreal, and G. Delgado-Barrio, Mol. Phys. **100**, 3231 (2002).
[52]MOLPRO, a package of *ab initio* programs designed by H.-J. Werner and P. J. Knowles, version 2009.1, R. D. Amos, A. Bernhardsson, A. Berning, *et al*.
[53]K. A. Peterson, D. E. Woon, T. H. Dunning, Jr., J. Chem. Phys. **100**, 7410 (1994).
[54]A. Jäckle and H.-D. Meyer, J. Chem. Phys. **104**, 7974 (1996).
[55]A. Jäckle and H.-D. Meyer, J. Chem. Phys. **109**, 3772 (1998).
[56]X. Chapuisat, A. Belafhal, and A. Nauts, J. Mol. Spectrosc. **149**, 274 (1991).
[57]H.-G. Yu, J. Chem. Phys. **117**, 2030 (2002).
[58]H.-G. Yu, J. Mol. Spectrosc. **256**, 287 (2009).